Contents lists available at ScienceDirect

Comptes Rendus Palevol

www.sciencedirect.com

General Palaeontology, Systematics, and Evolution (Intervetebrate Palaeontology)

Alveolina-dominated assemblages in the early Eocene carbonates of Jaintia Hills, NE India: Biostratigraphic and palaeoenvironmental implications

*Assemblages à dominance d'*Alveolina *dans les carbonates des Jaintia Hills, Nord-Est de l'Inde : biostratigraphie et implications paléoenvironnementales*

Suman Sarkar [a,b,*]

[a] *Birbal Sahni Institute of Palaeosciences, 53 University Road, 226007 Lucknow, India*
[b] *School of Earth Sciences, University of Bristol, Wills Memorial Building, Queens Road, BS8 1RJ Bristol, UK*

A B S T R A C T

Larger benthic foraminifera (LBF) are significant proxies in biostratigraphy and also act as excellent indicators of shallow-marine carbonate environments in fossil series. The Palaeogene LBF recorded from Meghalaya, NE India (eastern part of the relic eastern Tethys/Neo-Tethys) have high potential for dating shallow-marine sediments and documenting the multiple episodes of carbonate sedimentation that have contributed to the development of the Sylhet Limestone Group. Early Eocene witnessed the proliferation of LBF species worldwide, the phenomenon better known as the Larger Foraminiferal Turnover (LFT). Genera like *Alveolina*, *Nummulites* and *Orbitolites* with broad species complexes thrived as the dominant LBF amidst numerous other taxa on the verge of extinction or only surviving as stable forms. The current study emphasizes on the biostratigraphic and palaeoenvironmental account of the early Eocene Umlatdoh Limestone successions outcropping in the Jaintia Hills of Meghalaya, primarily based on the recorded species of *Alveolina* and other larger benthic foraminifera. Five species of *Alveolina* — *A. oblonga*, *A. schwageri*, *A.* cf. *ruetimeyeri*, *A.* aff. *haymanensis* and *A.* aff. *varians* are recorded in the evaluated sections that indicate an early Eocene age corresponding to the Shallow Benthic Zone 10. Major carbonate facies types in the present assessment include oolitic-smaller benthic foraminiferal -green algal grainstone–packstone, smaller miliolid-*Alveolina* grainstone, green algal-benthic foraminiferal grainstone, larger porcellaneous (*Alveolina*) grainstone-packstone, *Alveolina*-nummulitid grainstone-rudstone, and nummulitid grainstone-rudstone, which indicate a shallow marine, high-energy depositional environment ranging from shoal-sandy bars to a distal inner ramp setting.

© 2019 Académie des sciences. Published by Elsevier Masson SAS. All rights reserved.

R É S U M É

Les plus grands foraminifères benthiques (LBF) sont des *proxies* significatifs en biostratigraphie et aussi d'excellents indicateurs d'environnements carbonatés marins de faible profondeur dans les séries fossiles. Le registre LBF du Paléogène de Meghalaya, dans le

* Correspondance to: Birbal Sahni Institute of Palaeosciences, 53, University Road, 226007 Lucknow, India.
 E-mail addresses: suman763@gmail.com, suman.sarkar@bristol.ac.uk

Nord-Est de l'Inde (partie orientale de la Téthys orientale/Néo-Téthys relique), présente un fort potentiel pour dater les sédiments marins de faible profondeur et pour documenter les multiples épisodes de sédimentation carbonatée qui ont contribué au développement du Sylhet Limestone Group. L'Éocène inférieur témoigne de la prolifération des espèces du LBF, le phénomène mieux connu sous le nom de *Large Foraminiferal Turnover*. Des genres comme *Alveolina*, *Nummulmites* et *Orbitulines*, avec de nombreuses espèces, prospèrent en tant que LBF prédominants au sein de multiples autres taxons qui sont au bord de l'extinction ou ne survivent que sous des formes stables. L'étude actuelle souligne la valeur biostratigraphique et paléoenvironnementale de l'Éocène inférieur des successions de calcaire d'Umlatdoh, qui affleurent dans les Jaintia Hills de Meghalaya, antérieurement basées sur les espèces collectées d'*Alveolina* et autres grands foraminifères benthiques. Cinq espèces d'*Alveolina*–*Alveolina oblonga*, *A. schwageri*, *A.* cf. *ruetimeyeri*, *A.* aff. *haymanensis* et *A.* aff. *varians* sont enregistrées dans les coupes évaluées comme étant d'âge Éocène inférieur correspondant à la *Shallow Benthic Zone* 10. Les principaux types de faciès carbonatés incluent des *grainstone-packstone* à petits foraminifères benthiques et algues vertes — des *grainstones* à petits miliolidés-*Alveolina*, des *grainstones* à foraminifères benthiques et algues vertes, des *grainstones-packstones* porcelanés (*Alveolina*), des *grainstones-rudstones* à *Alveolina* — nummulitidé et des *grainstones* à nummulitidé, qui indiquent un environnement dé dépôt de haute énergie dans une mer de faible profondeur, entre hauts-fonds sableux et rampe distale interne.

1. Introduction

The Eocene (56–33.9 Ma) is a critical period in the earth's geological history with respect to the climate evolution during the Cenozoic. The Eocene environments are defined by higher global temperatures in comparison to other periods of the Cenozoic (Greenwood and Wing, 1995; Huber and Caballero, 2011; Zachos et al., 2008). This epoch at the onset witnessed a distinct warming event at the Palaeocene–Eocene boundary, better known as the Palaeocene–Eocene Thermal Maximum (PETM) superimposed on a global greenhouse climate, followed by the Eocene Thermal Maximum 2 (Wing et al., 1995; Zachos et al., 2008). Later, the temperatures decreased to a long-lived climatic optimum in the middle Eocene followed by "ice-house" conditions with transient ice-sheets in the early Oligocene (Eldrett et al., 2009; Zachos et al., 2008). During the Eocene, larger benthic foraminifera (LBF) were one of the most important carbonate producers in shallow-marine tropical ecosystems (Kiessling et al., 2003; Pomar et al., 2017). The alveolinid, nummulitid, and orthophragminid species form the major basis for the shallow benthic zonations (SBZs) with regard to the Palaeogene platform and pelagic sequences of the western Tethys (Serra-Kiel et al., 1998). This scheme is primarily based on the extensive works dealing with the alveolinids and nummulitids by Hottinger (1960) and Schaub (1981). These SBZs have been applied successfully for high-resolution biostratigraphy in various shallow-marine environments, strongly dominated by LBF in the Palaeocene and the Eocene (Drobne et al., 2011; Scheibner and Speijer, 2009; Scheibner et al., 2005, 2007). However, studies linking and correlating these western Tethyan SBZs to the eastern Tethyan environments have not been carried out barring a few investigations (Afzal et al., 2011; BouDagher-Fadel et al., 2015; Zhang et al., 2013).

LBF are highly abundant, diverse and widely distributed benthic groups dwelling in shallow-marine conditions and applied as an excellent tool in biostratigraphic studies along with the reconstruction of palaeoenvironments (Beavington-Penney and Racey, 2004; BouDagher-Fadel et al., 2015; Matsumaru and Sarma, 2010; Özgen-Erdem et al., 2007; Pomar et al., 2017; Sarkar, 2015, 2016, 2017a, 2019; Scheibner and Speijer, 2009; Scheibner et al., 2007). LBF are abundant in numerous shelf carbonate settings, covering a wide array of platform environments. A wide range of abiotic (temperature, salinity, depth, dissolved oxygen, inorganic trophic resources, plate tectonics) and biotic (biogeography, organic trophic resources, adaptive radiation, convergent/divergent evolution, rates of extinction) factors influence the distribution of LBF taxa, sometimes producing an individual impact or in several instances acting in tandem (Briguglio and Hohenegger, 2011; Hallock and Glenn, 1986; Hottinger, 1982, 1997; Renema, 2008; Scheibner et al., 2005). LBF have been a principal fossil group for Palaeogene biostratigraphy applicable to the Tethyan realm, such as the Palaeogene of northeastern India (Jauhri and Agarwal, 2001; Matsumaru and Sarma, 2010). Meghalaya situated in the present northeastern India was palaeogeographically located at the eastern margins of the Tethyan Ocean during the Early Palaeogene, and acted as a site for the deposition of large volumes of shallow-marine carbonates. Palaeontological and biostratigraphical studies on carbonate platform successions from the Sylhet Limestone Group, NE India have documented a great diversity of shallow-marine LBF corresponding to the late Palaeocene to the middle Eocene (Jauhri, 1994, 1997, 1998; Jauhri and Agarwal, 2001; Kalita and Gogoi, 2015; Matsumaru and Sarma, 2010; Sarkar, 2015a, 2016, 2017, 2019). Although it corresponds to a very important time slice of the geological record, the Umlatdoh Limestone has not received substantial attention for comprehensive

analyses of the LBF in the biostratigraphic perspective, in comparison to the Lakadong Limestone (lowermost) and Prang Formation (upper) of the Sylhet Limestone Group.

The major objective of this study is to provide a brief biostratigraphic account of the *Alveolina* species from the early Eocene shallow-marine successions outcropping in the Lumshnong area of the Jaintia Hills in Meghalaya, northeastern India, and to make an inference on their palaeoecological implications. Hottinger (1960) presented the first comprehensive biostratigraphic account of the genus *Alveolina* describing eight biozones in the early Eocene (Ypresian) based on data from the Tethyan province. Another detailed analysis related to the biostratigraphic zonation of the alveolinids was carried out by Serra-Kiel et al. (1998), describing twenty shallow benthic zones (SBZs). The origin and diversification of the alveolinid taxa during the Palaeogene represent a classic example of anagenesis (evolution within a single lineage) dominating over cladogenesis (branching evolutionary pattern). *Alveolina* has developed a single kind of test structure related to its entire spatiotemporal range. Within *Alveolina*, one characteristic is uniform in function through geological time (shape of shell; spire) while traits like the proloculus size and the index of elongation have undergone several modifications.

This paper also presents a detailed account of the early Eocene LBF assemblages well dominated by *Alveolina* and the major facies types (MFTs) corresponding to the Umlatdoh Limestone. A preliminary baseline study of the microfacies types and Ypresian palaeoenvironment related to the Umlatdoh Limestone sections from this locality has recently been provided by Kalita and Gogoi (2015). However, there is a need for further analysis with respect to the critical aspects of LBF biostratigraphy and palaeoecology. In the present study, all the examined sections comprise variable species of *Alveolina* acting as important carbonate facies components. Changes in the relative abundance of various microfacies components across the evaluated successions provide interesting insights into the palaeoenvironmental reconstruction of the study area. These data contribute to the knowledge on the alveolinid and other foraminifers dominant in the locality during the early Eocene with precise biostratigraphic and palaeoecological implications.

2. Geological setting

Assam Shelf comprises the Jaintia, Khasi, Garo, Mikir Hills, Shillong Plateau, and the upper Assam Valley, representing the northeastern extension of the Indian Craton. Incessant tectonic activity along the Himalayan and the Arakan–Yoma fault zones, followed by the Indo-Asia plate collision, regulated the platform development in the area (Jauhri and Agarwal, 2001; Murty, 1983). Late Cretaceous witnessed the advent of platform conditions in the region with a beginning of sandstone deposition. The clastic sedimentation carried on till the early Palaeocene, but a late Palaeocene large-scale modification in the tectonic regime reduced the subsidence rates that led to a significant decrease in the clastic material supply to the depositional area. This eventually resulted in the formation of the carbonate platform upon which the sequences belonging to the Sylhet Limestone Group were deposited. The carbonate platform persisted till the late middle/late Eocene, when a further significant modification in the tectonic regime resulted in a rapid inflow of terrigenous clastic material leading to the deposition of thicker clastic sediments during the Late Palaeogene and the Neogene (Jauhri and Agarwal, 2001).

A widespread and prolonged marine transgression phase, occasionally interrupted by an increase in clastic supplies and shallowing cycles laid down the deposits of the Sylhet Limestone Group (Jauhri and Agarwal, 2001). The depositional type in the carbonate platform environment tended to become reefal throughout the course of development of the Sylhet Limestone (Ghose, 1976; Jauhri, 1994; Jauhri and Agarwal, 2001). Nagappa (1959) used LBF as biostratigraphic proxies to document subdivisions of the Sylhet Limestone Group based on random thin-section study. He presented their correlation with the Ranikot, Laki, and Khirthar (= Kirthar) stages of Pakistan. Numerous Tethyan fauna (Hottinger, 1960; Hottinger and Drobne, 1988; Matsumaru, 1996; Racey, 1995) have been reported from the Sylhet Limestone Group, which facilitates precise correlation with the European stages (Jauhri, 1997, 1998; Jauhri and Agarwal, 2001).

The Sylhet Limestone Group encompasses three carbonate litho-units–Lakadong Limestone, Umlatdoh Limestone and Prang Formation in ascending chronological order intercalated with the Lakadong Sandstone and Narpuh Sandstone (Dasgupta, 1977; Jauhri and Agarwal, 2001). Sylhet Limestone Group is underlain by the upper Danian to Selandian Therria Sandstone and overlain by shale/sandstone alternations of the Priabonian Kopili Formation (Jauhri and Agarwal, 2001; Sarma et al., 2014). Umlatdoh Limestone lies between the Lakadong Sandstone and the Narpuh Sandstone. Lumshnong and its adjoining localities represent the most complete section of the entire Sylhet Limestone Group (Kalita and Gogoi, 2015). The successions corresponding to the early Eocene Umlatdoh Limestone in the Lumshnong area encompass hard, massive, and extremely thick carbonates in association with dolomites, shales, and sandstones.

3. Material and methods

For the present study, fieldwork was carried out in the Topcem Cement Factory premises (92°23.3′E; 25°12.5′N) located in Lumshnong within the Jaintia Hills, Meghalaya (Fig. 1). Three limestone sections from Mine No.3 of the Topcem establishment (Fig. 2) were measured (Section 1, 7 m; Section 2, 9 m; Section 3, 9.5 m) and 52 limestone samples have been collected for the analysis of the LBF and their associated facies components (Figs. 3–5). The studied sections are characterized by dark grey to beige coloured limestones with intermittent carbonate–siliciclastic mixed layers. A total of 90 petrographic thin sections (~3.0–4.0 × 2.0–2.5 cm)
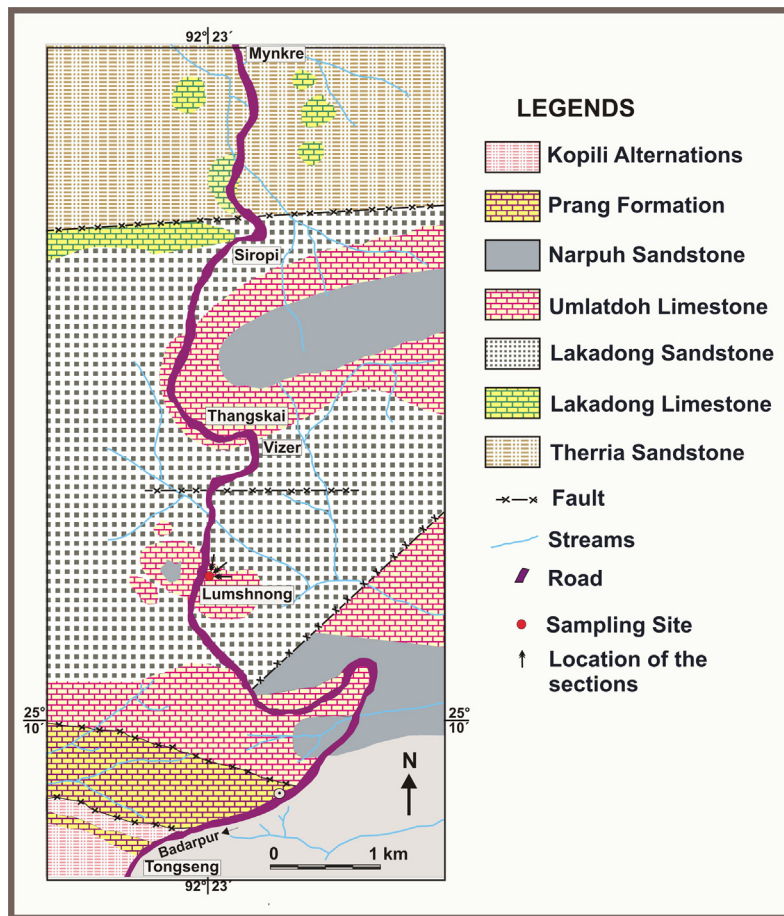
Fig. 1. Geological map showing the study area on the Jowai–Badarpur Road Transect (modified from Dutta and Jain, 1980).
Fig. 1. Carte géologique montrant la zone d'étude sur le transect de la route Jowai–Barpur (modifié d'après Dutta et Jain, 1980).
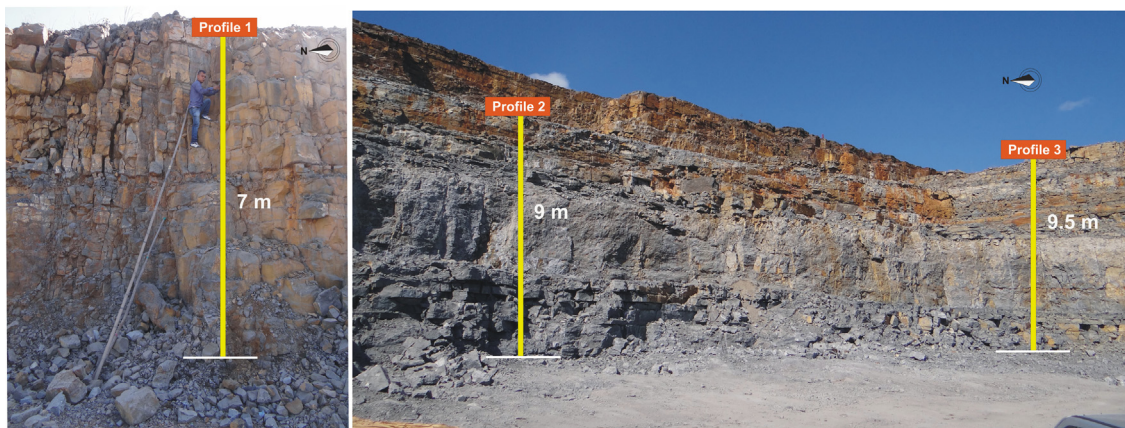

Fig. 2. Field photographs highlighting the studied sections in the Topcem cement factory establishment in the Jaintia Hills, Meghalaya (Mine No. 3).
Fig. 2. Photos de terrain, montrant les coupes étudiées dans l'usine de ciment de Topcem dans les Jaintia Hills, Meghalaya (Mine Nº 3).

were prepared for the identification of the skeletal components and evaluation of the carbonate textures. Taxonomic identifications of the foraminiferal tests were based on randomly oriented thin sections and when possible the recognized individuals have been identified at a generic or specific rank. The LBF specimens were analyzed at various magnifications ($4\times$–$40\times$) to evaluate their test structure and possible ecological affinities in relation to the other biotic components. The relative abundances of the LBF and other fossil biota
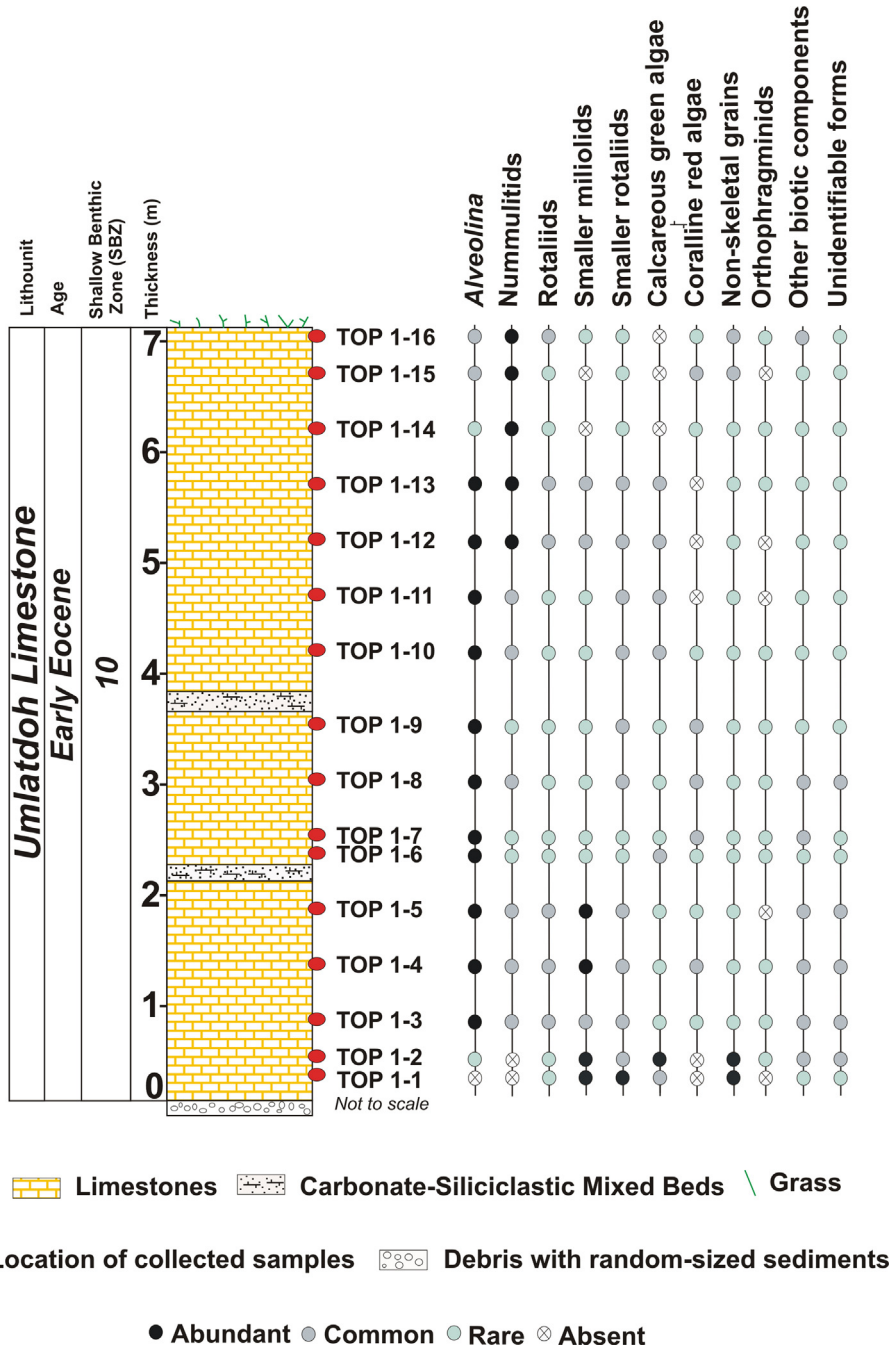
Fig. 3. Lithocolumn of section 1 studied showing the major skeletal/non-skeletal components and their relative abundance with locations of collected samples.

Fig. 3. Colonne lithostratigraphique de la coupe 1 étudiée, montrant les principaux composants squelettiques et non squelettiques et leur abondance relative avec les localisations de collecte des échantillons.

were estimated in the thin sections by image analysis and by measuring the proportional area occupied by each taxon relative to the total biotic population (Perrin et al., 1995). The material used for this study is housed in the Birbal Sahni Institute of Palaeosciences, Lucknow, India.

4. Results and discussion

4.1. Biotic diversity

Biotic components of the studied material include dominant benthic foraminifera, both small and larger, in
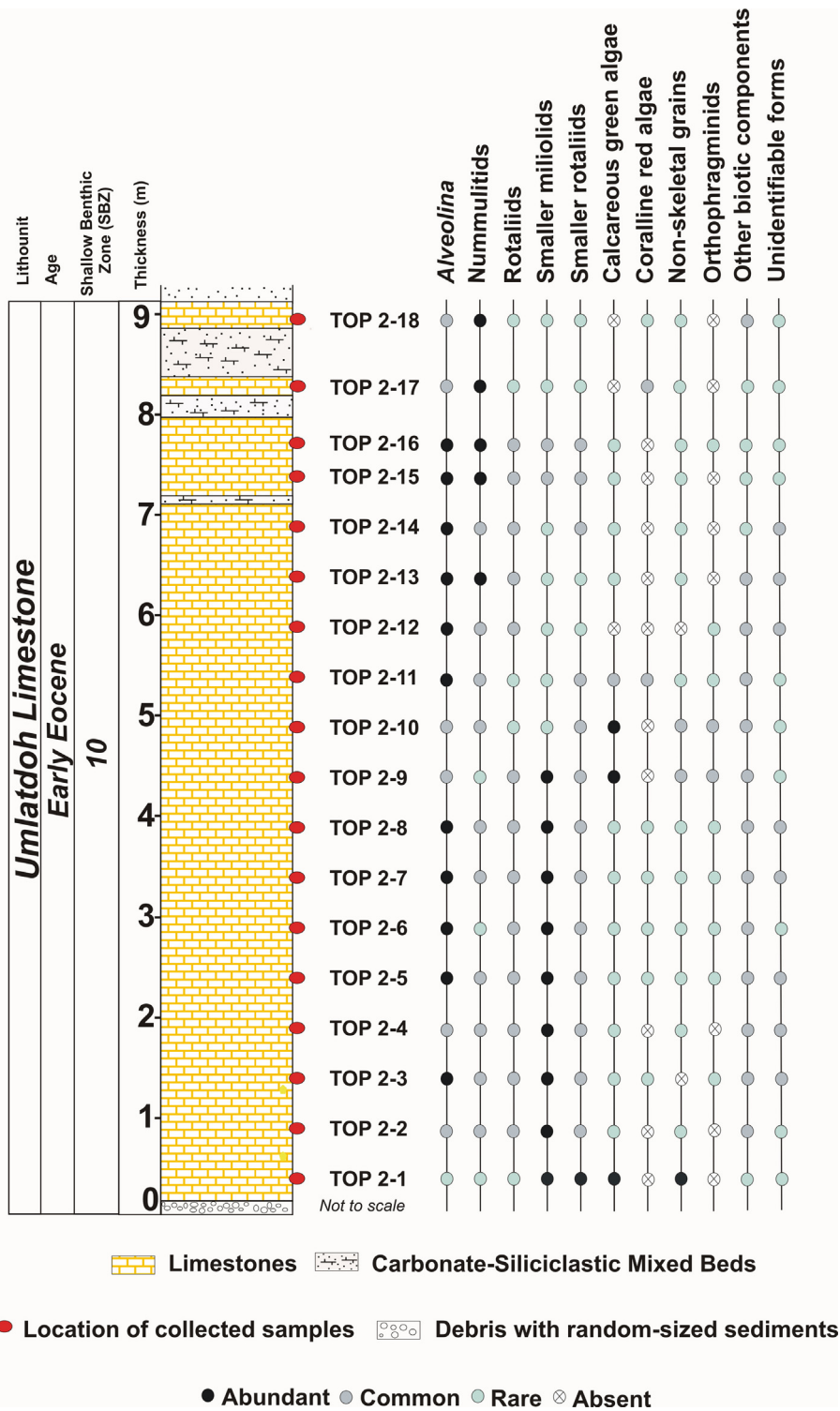
Fig. 4. Lithocolumn of section 2 studied showing the major skeletal/non-skeletal components and their relative abundance, with the locations of the collected samples.
Fig. 4. Colonne lithostratigraphique de la coupe 2 étudiée, montrant les principaux composants squelettiques et non squelettiques et leur abondance relative, avec les endroits de collecte des échantillons.
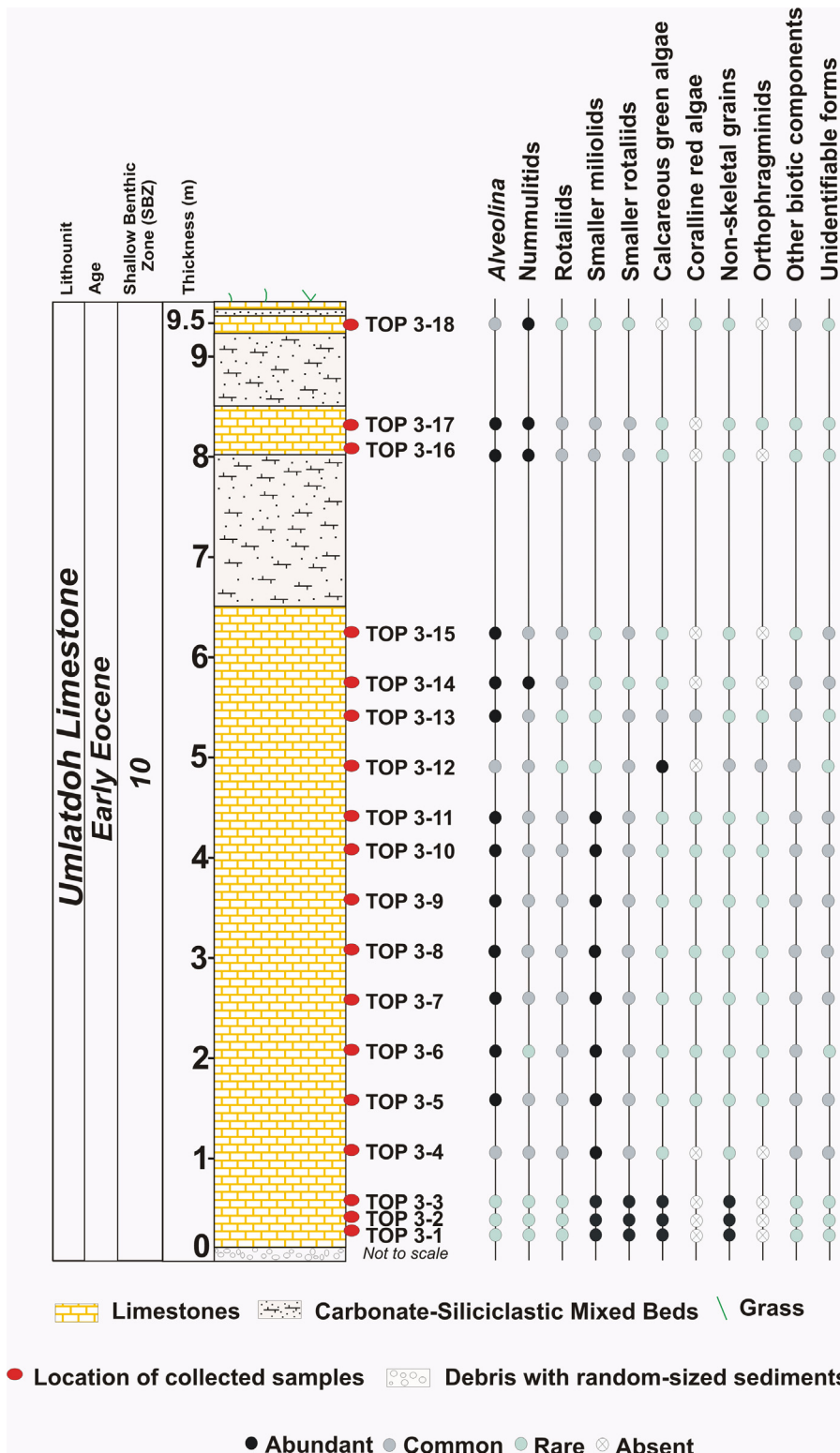
Fig. 5. Lithocolumn of section 3 studied showing the major skeletal/non-skeletal components and their relative abundance with locations of collected samples.
Fig. 5. Colonne lithostratigraphique de la coupe 3 étudiée, montrant les composants squelettiques et non squelettiques et leur abondance relative, avec les endroits de collecte des échantillons.
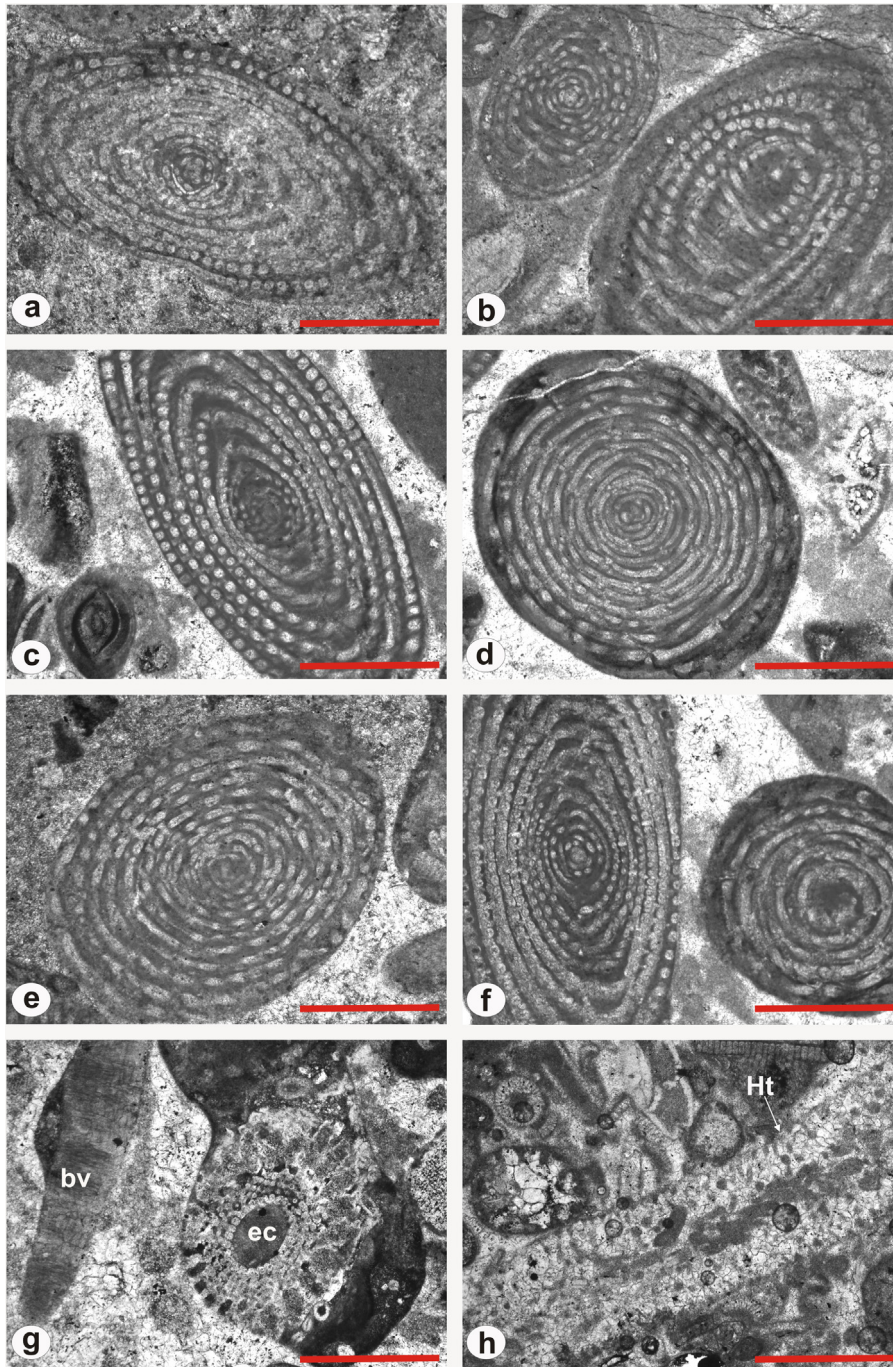
Fig. 6. Microphotographs representing the major facies components: a: *Alveolina oblonga*, sample No. TOP 1-8; b: *Alveolina oblonga* and another alveolinid, sample No. TOP 2-9; c: *Alveolina oblonga, sample* No. TOP 1-7; d: *Alveolina schwageri*, sample No. TOP 2-12; e: *Alveolina* cf. *ruetimeyeri*, TOP 3-11; f: *Alveolina* aff. *haymanensis*, sample No. TOP 2-11; g: A bivalve shell fragment (bv) and echinoid spine (ec), sample No. TOP 2-9; h: *Halimeda tuna* (Ht) with ooids and other algal fragments, sample No. TOP 1–12. Scale bars: a: 1.5 mm; b: 2 mm; c: 1 mm; d: 0.5 mm; e: 1.5 mm; f: 2 mm; g–h: 0.5 mm.
Fig. 6. Microphotographies représentant les principaux composants des faciès : a : *Alveolina oblonga*, éch. nᵒ TOP 1-8 ; b : *Aleveolina oblonga* et un autre alvéolinidé, éch. nᵒ TOP 2-9 ; c : *Alveolina oblonga,* éch. nᵒ TOP 1-7 ; d : *Alveolina schwageri,* éch. nᵒ TOP 2-12 ; e : *Alveolina* cf. *ruetimeyeri*, éch. nᵒ TOP 3-11 ; f : *Alveolina* aff. *haymanensis*, éch. TOP 2-11 ; g : fragment de coquille de bivalve (bv) et épine d'échinoïde (ec), éch. nᵒ TOP 2-9 (H) *Halimeda tuna* (Ht), avec ooïdes et autres fragments algaires, éch. nᵒ TOP 1–12. Barres d'échelle : a : 1,5 mm ; b : 2 mm ; c : 1 mm ; d : 0,5 mm ; e : 1,5 mm ; f : 2 mm ; g–h : 0,5 mm.
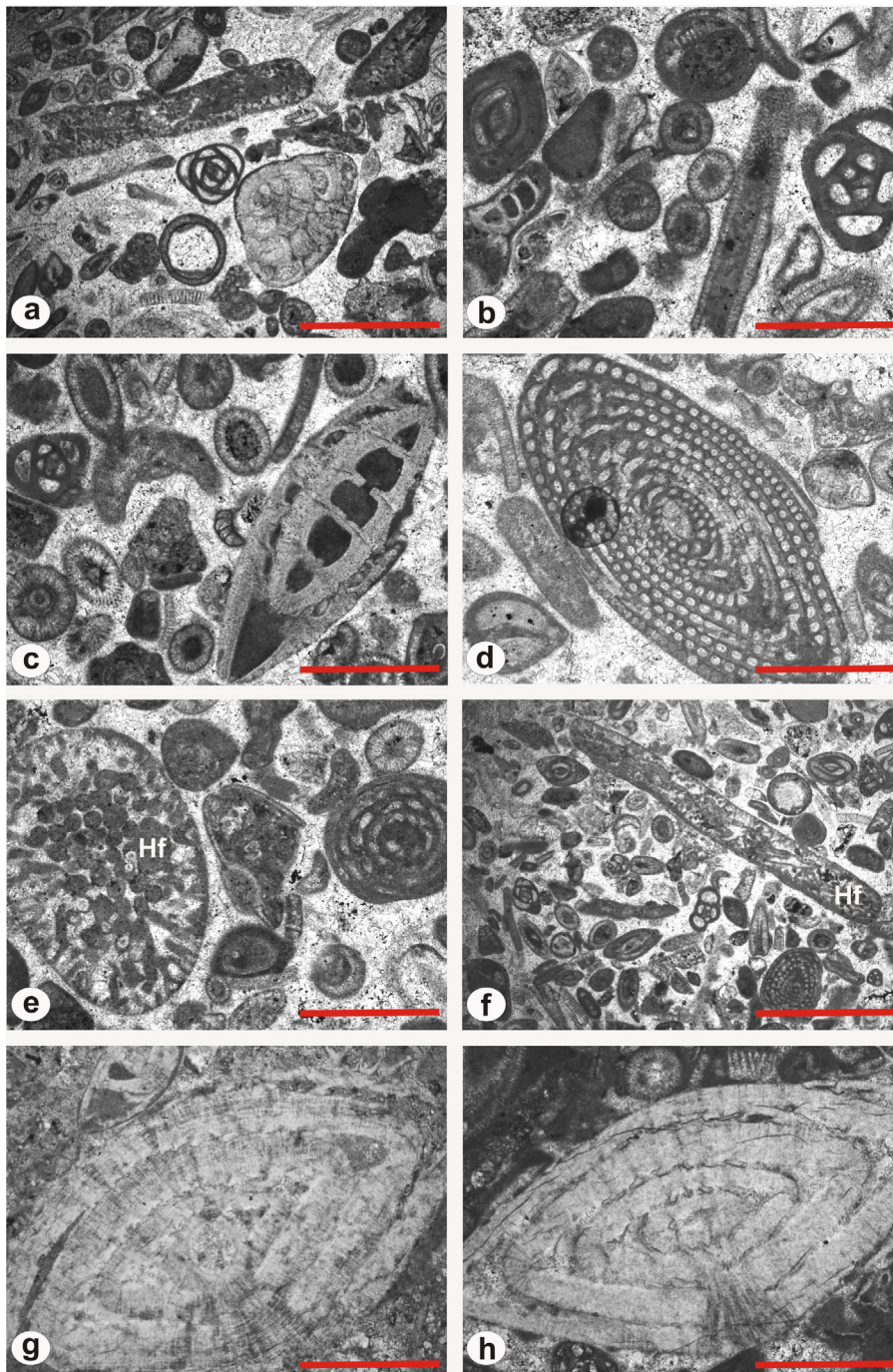
Fig. 7. Microphotographs representing the major facies components: a–c: ooids, coated grains, *Quinqueloculina* sp., *Halimeda* sp., *Daviesina* sp., *Assilina laxispira*, smaller miliolids and green algae in grainstone-packstone facies, sample Nos. TOP 2-1 (a and b), TOP 1-1 (c); d: *Alveolina* aff. *varians* with *Biloculina* sp. in grainstone facies, sample No. TOP 2-5; e and f: *Halimeda fragilis* (Hf) with dasyclads, ooids, smaller miliolids and glomalveolinid tests in grainstone matrix, sample No. TOP 2-9; g: *Nummulites burdigalensis* (axial section) with another smaller nummulitid in rudstone-grainstone facies, sample No. TOP 1-14; h: *Nummulites atacicus* (oblique section) in rudstone-grainstone facies, sample No. TOP 3-18. Scale bars: a–e: 1 mm; f: 2 mm; g–h: 0,5 mm.

Fig. 7. Microphotographies représentant les principaux composants des faciès : a–c : Ooïdes et grains recouverts, *Quinqueloculina* sp. *Halimeda* sp., *Daviesina* sp., *Assilina laxispira*, les plus petits milliolidés et algues vertes dans le faciès *grainstone-packstone*, éch. n° TOP 2-1 (a et b), TOP 1-1 (c) ; d : *Alveolina* aff. *varians* with *Biloculina* sp. dans le faciès *grainstone*, éch. n° TOP 2-5; e et f : *Halimeda fragilis* (Hf) avec dasyclades, ooïdes, tests de petits milliolidés et glomalveolinidés dans la matrice du *grainstone*, éch. n° TOP 2-9 ; g : *Nummulites burdigalensis* (section axiale) avec un autre petit nummulidé dans le faciès *rudstone-grainstone*, éch. TOP 1-14 ; h : *Nummulites atacicus* (section oblique) dans le faciès *mudstone-grainstone*, éch. TOP 3-18. Barres d'échelle : a–e : 1 mm ; f : 2 mm ; g–h : 0,5 mm.
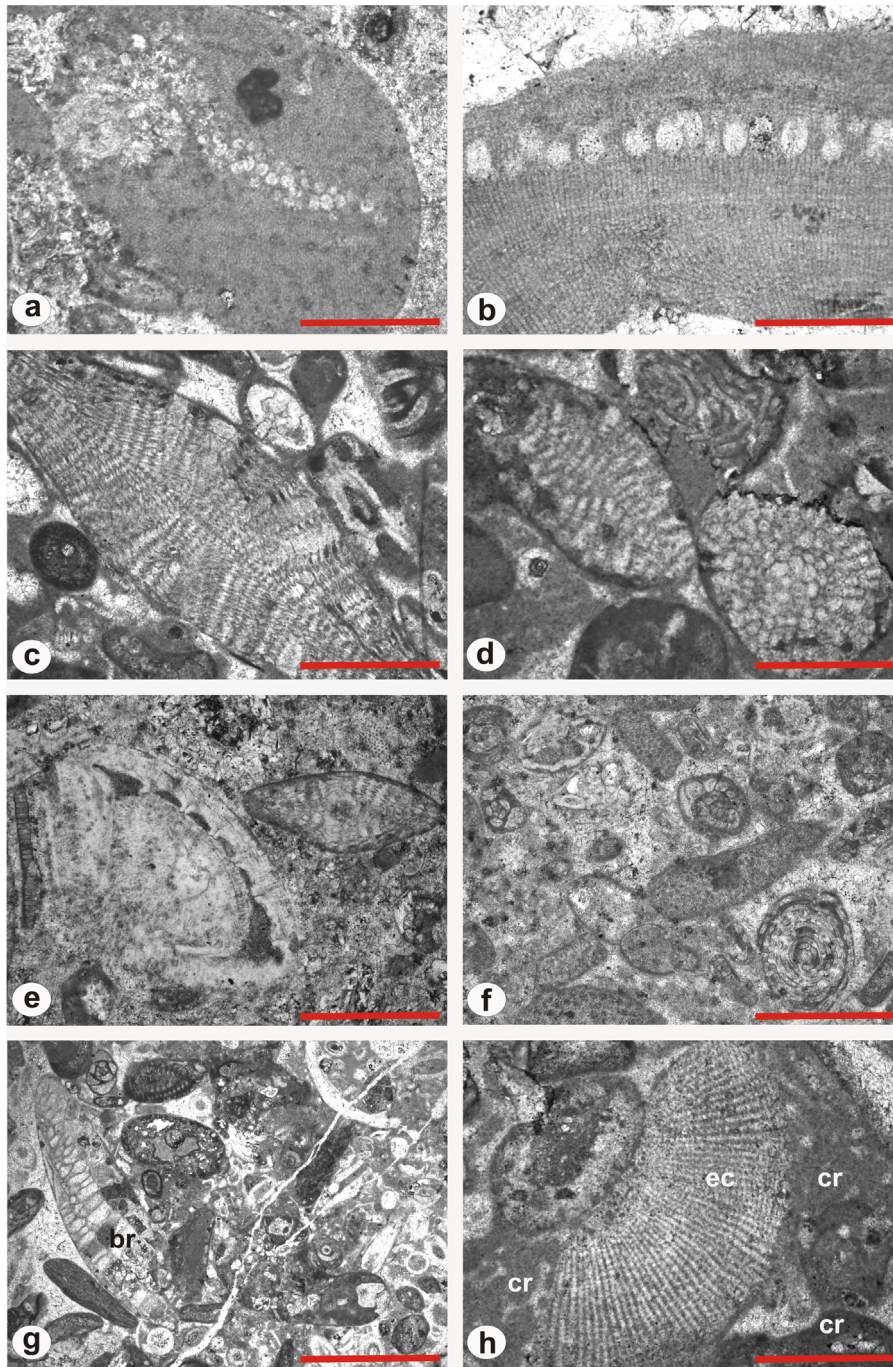
Fig. 8. Microphotographs representing the major facies components: a and b: *Sporolithon* spp. showing (a) a warty protuberance influenced by abrasion/bioerosion, sample No. TOP 1-8, and (b) unconsolidated thallus, sample No. TOP 3-13; c and d: Orthophragminid *Discocyclina* in grainstone matrix, sample Nos. TOP 1–7 (c) and TOP 1-9 (d); e: *Lockhartia* sp. with an orthophragminid (*Discocyclina*?) in packstone matrix, sample No. TOP 1-13; f: *Neorotalia* sp. with smaller benthic foraminifera, green algae and alveolinids in grainstone facies, sample No. TOP 2-6; g: bryozoan fragment (br) with smaller benthic foraminifera, coralline red algal debris and coated grains in grainstone-packstone facies, sample No. TOP 3-5; h: echinoid plate (ec) with coralline red algae (cr), sample No. TOP 3-13. Scale bars: a–c: 0,5 mm; d: 1 mm; e: 0,5 mm; f: 2 mm; g: 1 mm; h: 0,5 mm.

Fig. 8. Microphotos représentant les principaux composants des faciès : a : *Sporolithon* spp. montrant (a) une protubérance véruqueuse influencée par abrasion/bioérosion, éch. nº TOP 1-8 et (b) thallus non consolidé, éch. nº TOP 3-13 ; c et d : orthophragminidé *Discocyclina* dans la matrice de *grainstone*, éch. TOP 1-7 (c) et TOP 1-9 (d) ; e : *Lockhartia* sp. avec un orthophragminidé (*Discocyclina*?) dans la matrice de *packstone*, éch. nº TOP 1-13 ; f : *Neorotalia* sp. avec de petits foraminifères benthiques, des débris d'algues vertes et des alvéolinidés dans le faciès *grainstone*, éch. nº TOP 2-6 ; g : fragment de bryozoaire (br) avec de petits foraminifères benthiques, des débris d'algues coralliennes et des grains recouverts dans le faciès *grainstone-packstone* (cr), éch. nº TOP 3-5 ; h : plaque d'échinoïde (ec) avec des algues rouges coralliennes, éch. nº TOP 3-13. Barres d'échelle : a–c, 0, 5 mm ; d : 1 mm ; e : 0,5 mm ; f : 2 mm ; g : 1 mm ; h : 0,5 mm.

association with calcareous green algae. Some major skeletal components of the evaluated carbonates assignable to the Umlatdoh Limestone including the species of *Alveolina* are shown in Figs. 6–8. Species of *Alveolina–A. oblonga* (Fig. 6a–c), *A. schwageri* (Fig. 6d), *A.* cf. *ruetimeyeri* (Fig. 6e), *A.* aff. *haymanensis* (Fig. 6f) and *A.* aff. *varians* (Fig. 7d) are the most widely distributed biotic components of the studied successions. Larger benthic foraminifera are common to abundant biogenic components in all the samples, except few (TOP 1-1, TOP 1-2, TOP 2-1, TOP 3-1, TOP 3-2 and TOP 3-3) rich in ooids, coated grains and smaller benthic foraminifera. Coralline red algae mainly represented by sporolithaceans (Fig. 8a–b), echinoid spines (Fig. 6g) and plates (Fig. 8h), gastropod and bivalve shells (Fig. 6g), bryozoans (Fig. 8g), encrusting foraminifera (acervulinids and planorbulinids), ostracods, serpulids and fragmented/abraded indeterminate bioclasts are also present across the sections but recorded only as secondary facies components. Ooids are present as the most abundant non-skeletal components of the studied sections. Small benthic foraminifera (SBF) include porcellaneous (miliolids), perforated (rotaliids) and agglutinated (textulariids) forms. The Umlatdoh Limestone comprises abundant small miliolids represented by *Quinqueloculina*, *Triloculina*, *Biloculina*, *Spiroloculina* and *Periloculina*. Rotaliids feature both planoconvex forms such as *Rotalia* and well-ornamented forms like *Daviesina* (Fig. 7a), *Lockhartia* (Fig. 8e) and *Neorotalia* (Fig. 8f). Agglutinated foraminifera are represented by rare to common well-preserved, seriate forms such as textulariids. LBF forms comprise porcellaneous taxa such as *Alveolina*, *Glomalveolina* and *Orbitolites* along with hyaline-lamellar taxa like *Discocyclina* and nummulitids (*Nummulites*, *Assilina* and *Operculina*). Larger orthophragminids like *Discocyclina* (Figs. 8c–e) are recorded in several samples. Calcareous green algae show considerable frequency in the studied material (Figs. 6g–h, 7a–b, e–f), including segments and plates of *Halimeda* (*H. tuna*, Fig. 6h; *H. fragilis*, Figs. 7e–f) and *Ovulites* with several dasycladalean fragments. Coralline red algae are represented by *Sporolithon* thalli in form of warty protuberances (Fig. 8a) and unconsolidated fragments (Fig. 8b), and algal debris constituted by abraded and fragmented thalli of geniculate and non-geniculate forms. Very rare reworked *Distichoplax* thalli are also observed. Non-geniculates (non-articulated corallines) are also present as very small nodules and protuberances not discernible at the generic level. Coralline red algae are frequently abraded and/or bioeroded, showing the influence of both strong hydrodynamic energy as well as other benthic organisms. Geniculate or the articulated forms are represented by very rare *Corallina* and *Jania*. These taxa were commonly diffused during the Cenozoic into very shallow ramp environments indicating bathymetric levels of less than 10 m (Brandano et al., 2009; Quaranta et al., 2012; Tomassetti et al., 2016).

4.2. Remarks on the biostratigraphy

In the evaluated Lumshnong sections, lower Eocene massive to cherty marly fossiliferous limestones are recorded, which correspond to the uppermost part of the Umlatdoh Limestone. These sections are characterized by abundant well-preserved benthic foraminifera that enable precise biostratigraphy. The occurrence of *Alveolina oblonga* (Figs. 6a–c) and of *A. schwageri* (Fig. 6d) with *Assilina laxispira* (Fig. 7c), *Nummulites burdigalensis* (Fig. 7g), *Nummulites globulus* and *N. atacicus* (Fig. 7h) assign an early Eocene (Cuisian) age corresponding to the SBZ10. *Nummulites atacicus* (SBZ 8) and *N. globulus* (SBZ 8-9) are both limited to earlier horizons of Eocene age according to Serra-Kiel et al. (1998), but other biostratigraphic studies have confirmed their range extension into deeper time even up to the Bartonian (Bieda, 1963; Ionesi, 1971; Massieux, 1973; Matsumaru and Sarma, 2010). The early Eocene (Cuisian) has been described by Hottinger (1960) as the *Alveolina oblonga* zone that stands equivalent to SBZ10 of Serra-Kiel et al. (1998). *A. oblonga* and *A. schwageri* are recorded most consistently in the studied samples, showing the highest frequency and abundance among all the LBF species, and found in the lowermost (except TOP 1-1) and topmost samples of all the sections, which confirms that the successions have deposited completely during the early Eocene. The SBZs can be well correlated with standard planktonic foraminiferal and calcareous nannoplankton zones (Papazzoni et al., 2017; Serra-Kiel et al., 1998; Zhang et al., 2018). This facilitates the construction of a high-resolution bio- and chronostratigraphy in carbonate sequences featuring LBF species. Owing to the complete absence of calcareous nannoplankton and planktonic foraminifera in the studied sections, any direct correlation with the recorded shallow benthic zone is constraining. However, based on literature survey and comparative studies, the currently studied sections assigned to the SBZ10 are correlated with calcareous nannoplankton zone NP12 and possibly planktonic foraminiferal zones P6b-P7 (Molina et al., 1992; Papazzoni et al., 2017; Pujalte et al., 2009; Schaub, 1981; Serra-Kiel et al., 1998).

Matsumaru and Sarma (2010) have reported Umlatdoh Limestone LBF assemblages from ridge sections outcropping in Nongkhlieh village of Shnongrim area, Jaintia Hills, Meghalaya. The presence of *Alveolina oblonga*, *A. schwageri*, *Assilina laxispira* and *A. placentula* as the major LBF in association with *Nummulites atacicus*, *N. burdigalensis*, *N. globulus* and *Alveolina globosa* indicated a correlation with the Laki Limestone of the Laki Stage of Sind area and the underlying Meting Limestone described by Nagappa (1959). A partial correlation was also established with LFA-2 and LFA-3 in the Indian Basins (Govindan, 2003), which is equivalent to the Letter Stage Tertiary a2 (Govindan, 2003; Matsumaru, 1996). The Umlatdoh Limestone assemblages as described by Matsumaru and Sarma (2010) have been ascribed to SBZs 7 to 11 (Fig. 9). An exception to this assignment is the presence of *Orbitolites complanatus*, which has a range from SBZ 12 (?) to SBZ 16 (?) and deserves further analysis. Sarkar (2016) has also reported larger benthic foraminifera from the lower part of the Umlatdoh Limestone assignable to SBZs 7-8 (middle Ilerdian) from a section located 2 km southeast of Lumshnong on the Jowai–Badarpur Road.

Fig. 9. Schematic chart showing the correlation between the latest version of the Eocene timescale (International Chronostratigraphic Chart 2019, http://www.stratigraphy.org) with the planktonic foraminiferal zones and the calcareous nannofossil zones (GTS 2012), and larger foraminiferal zones such as the Shallow Benthic Zones (updated version from Papazzoni et al., 2017), Indian Basin assemblages (Govindan, 2003), Haha-Jima, Japan (Matsumaru, 1996), Jaintia Hills in Meghalaya, NE India (Matsumaru and Sarma, 2010), and the Letter Stages (Matsumaru, 1996; Govindan, 2003). SBZ 10 has been highlighted to indicate the position of the sections in the current study.

Fig. 9. Charte schématique montrant la corrélation entre la dernière version de l'échelle des temps Éocène (International Chronostratigraphic Chart 2019, http://www.stratigraphy.org), avec les zones à foraminifères planctoniques et les zones à nanofossiles calcaires (GTS 2012), ainsi que les zones à plus grands foraminifères telles que les zones benthiques peu profondes (version mise à jour d'après Papazzoni et al., 2017), les assemblages du Bassin indien (Govindan, 2003), Haha-Jima, Japon (Matsumaru, 1996), Jaima Hills in Meghalaya, Nord-Est de l'Inde (Matsumaru et Sarma, 2010) et les *Letter Stages* (Govindan, 2003 ; Matsumaru, 1996). SBZ a été soulignée pour indiquer la position des coupes dans l'étude actuelle.

4.3. Microfacies and palaeoenvironmental analyses

All the carbonate microfacies recorded from the presently analysed Umlatdoh Limestone sections can be ascribed to a shallow-marine ramp environment. A general conceptual palaeoenvironmental model representing the depositional zones in the ramp environment and also the distribution of the major facies types are shown in Fig. 10. Whether these carbonate ramps were homoclinal or distally steepened in nature cannot be interpreted, since we are focusing on the shallowest environments. The studied limestone samples display low microfacies diversity and a

total of six major facies types (MFTs) were distinguished based on the carbonate texture and the dominant skeletal components. Most well-distributed, abundant components of the carbonate sedimentary samples are the larger foraminifers: alveolinids and nummulitids. Smaller miliolid, rotaliid and textulariid benthic foraminifera and diverse green algae (*Halimeda* with udotacean and dasycladalean forms) are found in association with the LBF species and show moderate abundance in the studied Umlatdoh Limestone microfacies. Abiotic ooids and coated grains are important non-skeletal components of the studied sections and are represented in variable
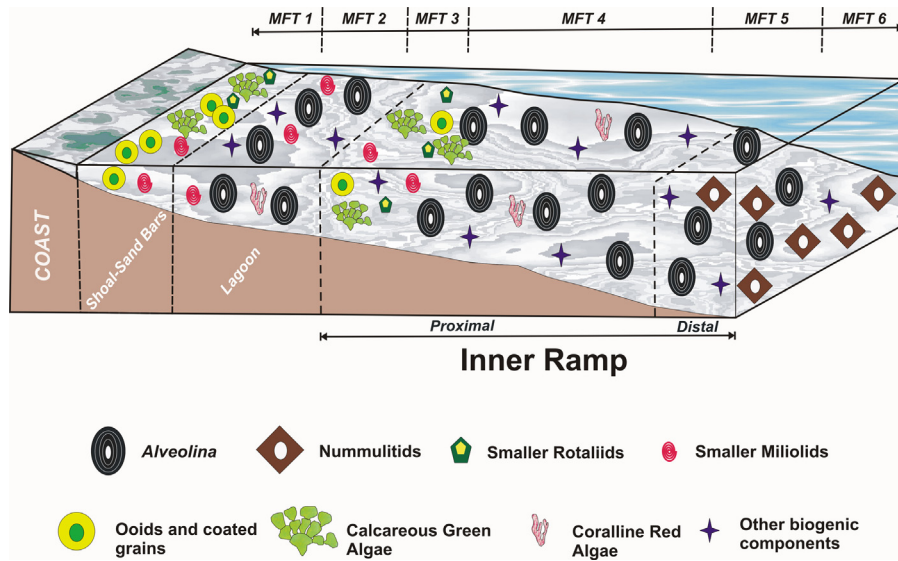
Fig. 10. A conceptual palaeoenvironmental model depicting the distribution of major facies components and types in the depositional environment with various zonations of the ramp setting.

Fig. 10. Modèle paléoenvironnemental conceptuel décrivant la distribution des principaux composants de faciès et les types d'environnement de dépôt avec les zonations variées d'établissement de la rampe.

abundance. Echinoderm plates and spines, partly broken and abraded gastropod and bivalve shells, small bryozoans fragments, coralline red algae mostly in form of small protuberances and debris, encrusting foraminifera (acervulinids and planorbulinids), ostracods, serpulids and fragmented/abraded indeterminate bioclasts occur across the different MFTs as subordinate facies components, but showing no considerable abundance in any of the samples/section.

MFT 1: Oolitic-smaller benthic foraminiferal-green algal grainstone-packstone (Fig. 7a–c)

This well-sorted microfacies varying in thickness from 0.35 to 1.0 m is recorded in the studied sections in form of oolitic bands and characterized by a high abundance of ooids and coated grains. The ooids feature concentric layering and possibly represent relics of radial structures. They are predominantly round in shape, with size varying from 0.15 to 0.6 mm. These are associated with varying proportions of smaller miliolids, rotaliids and green algae represented by *Halimeda* spp. followed by udotacean and dasycladalean forms. Subordinate components in this microfacies are peloids, algal fragments, echinoderm fragments and debris, intraclasts and aggregates also acting as the primary nuclei of the ooids and components of the coated grains. Some smaller miliolids, rotaliids, and textulariids unidentifiable up to the genus level are also observed in this microfacies. Rare alveolinids are also occasionally observed. Some unidentified sparite-filled bioclasts are also present. The matrix is generally sparite including few relics of micrite material. Drusy sparite and isopachous fibrous cement could be observed at several places around the ooids and coated grains.

Interpretation. This microfacies corresponds to a shoal environment (shoal-sand bar) influenced by tides and waves much above the normal wave base related to

depths < 10 m. The concentric ooids indicate high energy and normal marine salinity conditions that are well associated with a shoal setting in a shelf-edge or bank margin facies (Blendinger and Blendinger, 1989; Chablais et al., 2010). The near-total absence of mud and the occurrence of isopachous fibrous cement also indicate a high-energy depositional setting.

MFT 2: Smaller miliolid-*Alveolina* grainstone (Fig. 7d)

This poorly sorted microfacies with packstone matrix occurs only in the basal part of all the sections with thickness ranging from 0.8 to 2.5 m. MFT 2 is characterized by a high abundance of smaller miliolids (*Quinqueloculina*, *Triloculina*, *Biloculina*, *Spiroloculina*, and *Periloculina* species) in association with moderately abundant *Alveolina* (assemblages dominated by ovoid to slightly elongated A-forms–*Alveolina oblonga*, *A. schwageri*, *A.* aff. *varians* and several unidentifiable alveolinids). Some miliolid specimens showed resemblance to the genus *Pyrgo*, but the identification attempts were inconclusive. The grain size varies from 0.25 to 4.0 mm. The average diameter of *Alveolina* spp. in this microfacies is < 2 mm, but rare larger forms are recorded. Smaller nummulitids (*Nummulites* spp.), assilinids (*Assilina laxispira* and some indeterminate species) and rotaliids (*Lockhartia*, *Neorotalia, Daviesina*), textulariids (*Textularia*), orthophragminids, echinoid plates and spines, bivalve and gastropod shells, rare planorbulinid encrusting foraminifers, green algae, coralline red algal debris and *Sporolithon* thalli, serpulids and ooid grains are the subordinate facies components.

Interpretation. This MFT characterized by abundant smaller miliolids in association with larger *Alveolina* spp. indicates a restricted/protected lagoon to proximal inner ramp setting in a meso-oligotrophic nutrient regime with moderate to high hydrodynamic energy. The abundance of miliolids is an indication of warm, shallow-marine

depositional environment. They commonly develop habitats in both normal and hypersaline environments (Brasier, 1975; Chan et al., 2017; Gonera, 2012; Hottinger et al., 1993). Genera like *Quinqueloculina* and *Triloculina* are reported from multiple lagoonal environments in the Arabian Gulf (Amao et al., 2016; Murray, 1991), and their prolific occurrence in the studied carbonates indicates the deposition in a hypersaline environment (37–70‰) with water temperatures in the range of 16–40 °C (Murray, 1991), and bathymetric zonation from 12 to 18 m (Murray, 2006; Parker and Gischler, 2015).

The smaller miliolids are commonly categorized as r-strategist foraminifera showing short generation times, high fecundity, and rapid growth of populations (Reolid et al., 2014; Sarkar, 2015a). The abundance of these fauna indicates the possibility of adverse fluctuating environmental conditions where the limited amount of resources needs to be utilized as soon as they become available in the niche. Modern miliolids are euryhaline biota thriving on soft substrates corresponding to shallow restricted lagoon environments featuring low rates of turbulence (Zamagni et al., 2008). Alveolinids are very tolerant to a broad spectrum of temperature and salinity conditions, thereby facilitating their occurrence in various zones of shallow-marine carbonate platforms (Drobne et al., 2011; Hadi et al., 2018). Likewise, in the present case study, *Alveolina* spp. occurs throughout the section showing moderate to high abundance, thereby demonstrating a good degree of adaptability to various depositional environments. However, due to their symbiotic associations with microalgae as evidenced by several records (Hallock, 1985; Hohenegger, 2004, 2009), the entire successions are interpreted to have been deposited in shallow to very shallow water depths corresponding to the upper photic zone.

MFT 3: Green algal-benthic foraminiferal grainstone (Fig. 7e–f)

This poor-to-moderately-sorted microfacies with a packstone-grainstone matrix is 0.5–1.0 m in thickness and is dominated by calcareous green algae including multiple species of *Halimeda* (*H. fragilis*, *H. tuna*), udotacean genus *Ovulites* (*O. arabica*, *O. pyriformis*), and also various dasycladalean fragments. The benthic foraminiferal component of the MFT 3 is represented by *Alveolina*, smaller miliolids and rotaliids, smaller *Nummulites*, *Glomalveolina*, *Orbitolites*, *Discocyclina*, and encrusting forms like *Acervulina* and *Planorbulina*, and agglutinated *Textularia*. The grain size varies from 0.15 to 3.5 mm. *Halimeda* species are recorded in the form of segments and plates. Several small ooids and coated grains are dispersed throughout the microfacies and observed with few instances of isopachous fibrous cement. Gastropod and bivalve shells with ostracod, echinoderm, and bryozoan fragments are the other secondary components.

Interpretation. Calcareous green algae including dasycladalean and halimedacean forms are common constituents in early Eocene shallow-marine limestone sequences showing moderate/locally high abundance in the Umlatdoh Limestone (Sarkar, 2016). Green algae represent typical photozoan components that thrive in oligotrophic, well-illuminated waters facilitating photoautotrophy and photosymbiosis (Brandano et al., 2015;

Hallock and Schlager, 1986). However, there are some rare examples showcasing proliferation of green algae under increased nutrient inputs (Wilson and Vecsei, 2005). Lees (1975) described green-algae-dominated chloralgal assemblages in tropical, high-salinity areas (*Halimeda* shows broad salinity tolerance; 20–45‰). In a sharp contrast to its well-known status as a photozoan component sensitive to low light conditions, *Halimeda* has also been reported from deeper domains having low to very low light availability, for example the Hawaiian Islands, where it forms extensive meadows between depths of 65–120 m (Webster et al., 2006) and the Brazilian continental shelf extensively covered by rhodolith beds, where *Halimeda* is recorded from the intertidal zone to the 166-m bathymetric level (Amado-Filho et al., 2012; Bandeira-Pedrosa et al., 2004). The abundance of dasylcadalean forms with photosymbiotic LBF like *Alveolina* and *Nummulites* co-occurring with the *Halimeda* species strongly indicates the deposition of this microfacies in very shallow-water conditions (<20 m) related to the proximal inner ramp. A meso-oligotrophic nutrient regime is interpreted because nutrient-enriched conditions tend to reduce light penetration and decrease the availability of well-lit substrate expected to be a threshold requirement for this assemblage featuring calcareous green algae, smaller foraminifera and LBF.

MFT 4: Larger porcellaneous (*Alveolina*) grainstone-packstone (Fig. 6a–c, e–f)

This microfacies with grainstone-locally abundant packstone matrix shows a thickness of 2.5–3.0 m with unidirectional cross beddings and is characterized by moderate to poorly sorted large porcellaneous foraminifera mainly comprising subglobular to ovoid tests of *Alveolina* (> 40%; *Alveolina oblonga*, *A. schwageri*, *A.* aff. *haymanensis*, *A.* aff. *varians*) and several alveolinids not identifiable up to the species rank). The grain size ranges between 0.8 and 6.0 mm. The alveolinid tests show evidences of high hydrodynamic energy as the outer surface of youngest whorls is exfoliated, with truncated poles in numerous cases. Localized silt-sized sediments are also observed, dominated by calcisiltite. Subordinate biotic components of this microfacies are small nummulitids (A-form *Nummulites*), dasycladalean algae and *Halimeda* segments, non-geniculate algal protuberances (*Sporolithon* and mastophoroids), other small–medium-sized miliolids, orbitolids, smaller rotaliids, orthophragminids, acervulinids, echinoid remains and bryozoan fragments. Rare cortoids and peloids are also observed. Cement predominantly consists of drusy and blocky spar with isopachous to syntaxial cement. Several alveolinid tests are mildly abraded and rare cases of acervulinid encrustations on nummulitid tests are also recorded. A gently dipping planar to trough cross-bedded stratification can be observed in the case of this facies, with 1–2-m-thick individual units.

Interpretation. This grainstone-packstone facies is interpreted as representing bioclastic carbonate sandy shoals built in a shallow-marine, high-energy depositional setting influenced by wave processes in a nearshore inner ramp environment. Comparable unidirectional cross-bedding lithology has also been reported from numerous Cenozoic carbonate systems of Malta, Tunisia, and Italy

(Brandano et al., 2009; Loucks et al., 1998; Pedley, 1998; Tomassetti et al., 2016). The presence of dasycladalean and halimedacean green algae suggests a very shallow-water depositional setting (Wray, 1977). The occurrence of small biconvex A-forms of *Nummulites* tests along with subglobular to ovoidal alveolinids suggests a shallow-marine depositional setting corresponding to euphotic and oligotrophic conditions. Recent alveolinids have been reported from a plethora of marine habitats including deep lagoons to fore-reef sub-environments (Yordanova and Hohenegger, 2002). Living and fossil alveolinids are generally associated with shallow-marine settings, and their distribution depends primarily on light intensity and hydrodynamic conditions (Drobne et al., 2011; Tomassetti et al., 2016). Living larger miliolids like *Borelis* and *Alveolinella quoyi* do not dwell at depths > 50 m (Hohenegger, 1994, 2009; Langer and Hottinger, 2000). Their distributions are independent with respect to the substrate, which might have been any kind of algae, seagrasses or others (Beavington-Penney et al., 2006; Langer and Hottinger, 2000; Severin and Lipps, 1989). Thick carbonate successions encompassing rich populations of alveolinids were also interpreted to have deposited in lagoon or back-bank environments (Hottinger, 1977). Small, lens-shaped nummulitids have been envisaged to build habitats that share a common niche with alveolinids in the inner platform horizon (Geel, 2000). The abundance of A-form alveolinids with several tests presenting signs of abrasion in the outer walls, other porcelaneous forms (orbitolitids and miliolids), and also the presence of nummulitids and small rotalliids showing low quantitative numbers all indicate a deposition of this microfacies in the inner part of the ramp featuring high energy environments. A foraminiferal community dominated by *Alveolina* has been reported from Oman, which possibly thrived on the patchily vegetated muddy sands of a protected lagoon or embayment (Beavington-Penney et al., 2006). A fossil assemblage dominated by alveolinids, nummulitids, and orbitolitids from Turkey has been interpreted to have been deposited in a lagoon environment (Özgen-Erdem et al., 2005). *Alveolina*-dominated LBF assemblages have been linked to inner platform depositional environment, influenced by siliciclastic inputs in France (Rasser et al., 2005) and Spain (Scheibner et al., 2007).

MFT 5: *Alveolina*-nummulitid grainstone-rudstone (Fig. 6d)

This moderately sorted microfacies with packstone matrix is 1.5–2.0 m in thickness and is characterized by the predominance of *Alveolina* spp. (30–35%) including all the species recorded in the current study with small nummulitids with occasional larger *Nummulites* (15-20%) represented by *Nummulites burdigalensis* and *N. atacicus*. Subordinate components are tests of *Assilina*, *Daviesina*, *Lockhartia*, encrusting foraminifera (acervulinids and planorbulinids), udotacean green alga *Ovulites* and *Halimeda* spp., undetermined orthophragminids (*Discocyclina*?), textulariids, smaller miliolids and rotaliids, gastropod shells, echinoderm plates, and peloids.

Interpretation. This MFT is restricted to the proximal to distal inner ramp depositional setting and indicates a slightly deeper bathymetric level. MFT 5 actually represents a transitional phase between the very-shallow-water microfacies (MFTs 1 to 4) and comparatively deeper but overall shallow-water microfacies (MFT 6) where smaller miliolids and dasycladalean algae reduce drastically and larger foraminifers like *Alveolina*, *Nummulites* and others begin to show very high abundance. Beavington-Penney et al. (2006) reported a microfacies from the Eocene sediments of Oman showing a high degree of affinity with MFT 5, dominated by the species of *Alveolina*, *Nummulites*, and *Assilina*, corresponding to an inner ramp setting. The LBF *Assilina* is recorded in varying proportions throughout the presently studied succession, but never attains very high abundance levels. The nummulitid taxa are mostly observed in form of small, robust, broken/abraded A-form tests associated with medium-large sized *Alveolina* (*A. oblonga*, *A. schwageri, A.* cf. *ruetimeyeri*) within a packstone-locally grainstone matrix, that in combination with the factor of complete absence of dasycladalean green algae suggests deposition in the proximal to distal inner ramp with high hydrodynamic energy conditions. It is widely acknowledged that small and lenticular A-forms of *Nummulites* are more common in shallower inner ramp/shelf/platform settings (Beavington-Penney and Racey, 2004; Beavington-Penney et al., 2006; Hadi et al., 2018; Racey, 2001). Several examples of edgewise contact imbrications biofabrics also can be inferred as signatures of a high-energy depositional environment (Hadi et al., 2016, 2018). Numerous studies associated with the living and ancient LBF evidenced that, similarly to the currently studied successions, B-forms are rare or even completely absent in shallower horizons, whereas they are abundant at deeper depths (<100 m; Beavington-Penney et al., 2005; Hottinger, 1977).

MFT 6: Nummulitid grainstone-rudstone (Fig. 7g–h)

This microfacies is distinguished by a moderately sorted grainstone with the grain size ranging between 0.5 and 3.5 mm. The localized abundance of larger nummulitids (>2 mm) gives the impression of grainstones grading into rudstones at certain places. This facies is dominated by small to larger nummulitid taxa (*Nummulites*, *Assilina* and *Operculina*) with *Nummulites* (*N. globulus, N. atacicus*, *N. burdigalensis* and other indeterminate species) showing higher frequency. Additionally, encrusting acervulinids and planorbulinids, orthophragminids, smaller miliolids and rotaliids, *Halimeda*, coralline algal protuberances, echinoids, bryozoans, ostracods, rare serpulids and some larger alveolinids with syntaxial calcitic cement occur in a packstone-grainstone matrix. Small peloids and micritized cortoids are also observed. Among the nummulitids, the analysed assemblages are characterized by dominant A-forms. This microfacies does not display any clear sedimentary structure, with massive beds ranging from 1 to 1.5 m.

Interpretation. The nummulitid assemblages dominated by A-form *Nummulites* are interpreted as proximal inner-ramp palaeohighs impacted by winnowing and current processes. Various studies related to modern and ancient LBF indicate that the test morphology is controlled by a complex interaction of environmental factors such as light, depth, and water turbulence (Beavington-Penney and Racey, 2004; Eder et al., 2018; Hottinger, 1977, 1983;

Torres-Silva et al., 2019. Nummulitids are bottom-dwelling benthic fauna, and can be found at depths < 30 m, but usually dominant at mesophotic to oligophotic depths ranging at more than 30 m (Hohenegger, 2005; Španiček et al., 2017). Based on the ecophenotypical correlative studies with their modern counterparts, the nummulitids are associated with water depths between 40 and 80 m (Goeting et al., 2018; Hadi et al., 2016). However, in the current study, relative palaeobathymetric position of this microfacies is inferred to be much less than 40 m, at about 25–30 m due to the presence of green algae and smaller foraminifera with the abundant nummulitids. MFT 6 is relatively deeper in comparison to the other MFTs due to the prevalence of LBF tests and coralline algal protuberances with lesser fragmentation and abrasion (tests and algal thalli more compact in this microfacies), almost negligible isopachous fibrous cement and also an increase in the incidence of encrusting foraminifera (acervulinids and planorbulinids). Small and lenticular tests of *Nummulites* are more common in very shallow to shallow inner platform/shelf/ramp settings (Racey, 2001). The accumulations of A-form *Nummulites*-dominated assemblages with robust/ovate tests and rare B-forms suggest a shallow-marine inner ramp depositional environment affected by limiting conditions, for example, slightly higher nutrient levels, favouring the development of a community of r-strategists (Beavington-Penney and Racey, 2004; Beavington-Penney et al., 2005; Eder et al., 2016; Hadi et al., 2016).

5. Conclusions

Larger benthic foraminifers are important biotic components of the early Eocene Umlatdoh Limestone successions outcropping in the Lumshnong region of the Jaintia Hills, Meghalaya, northeastern India. The LBF assemblages are dominated by multiple species of *Alveolina* (*A. oblonga*, *A. schwageri*, *A.* cf. *ruetimeyeri*, *A.* aff. *haymanensis* and *A.* aff. *varians*). In addition to *Alveolina*, the studied assemblages also comprise various other foraminiferal genera like *Nummulites*, *Assilina*, *Operculina*, *Glomalveolina*, *Discocyclina*, *Lockhartia*, *Neorotalia*, *Daviesina*, *Textularia*, *Acervulina* and *Planorbulina*. A detailed analysis of the LBF (Species of *Alveolina* with *Nummulites* - *N. burdigalensis*, *N. globulus*, *N. atacicus* and *Assilina–A. laxispira*) indicates that these successions, corresponding to the upper part of the Umlatdoh Limestone, were deposited entirely during the early Eocene (SBZ 10 interval). Ooids, coated grains and calcareous green algae including species of *Halimeda*, *Ovulites* and multiple dasycladalean forms have also been recorded in low to abundant proportions in the analysed sections. Coralline red algae, echinoderms, bryozoans, gastropods and bivalves are other considerable biogenic components of the analysed microfacies. Based on the analyses of the carbonate microfacies and their fossil components, six major facies types are reported, which indicate that the depositional environment ranges from shoal-sandy bars to an inner ramp setting corresponding to shallow depths with high hydrodynamic energy within the upper photic zone. Diverse assemblages of LBF represent a phase of significant foraminiferal turnover in this region representing

the eastern part of the East Tethys and facilitate correlation studies with the West Tethyan fauna in order to understand the prospects for possible links across the Tethyan horizon.

References

Afzal, J., Williams, M., Leng, M.J., Aldridge, R.J., 2011. Dynamic response of the shallow marine benthic ecosystem to regional and pan-Tethyan environmental change at the Paleocene–Eocene boundary. Palaeogeogr. Palaeoclimatolol. Palaeoecol. 309, 141–160.

Amado-Filho, G.M., Moura, R.L., Bastos, A.C., Salgado, L.T., Sumida, P.Y., Guth, A.Z., Francini-Filho, R.B., Pereira-Filho, G.H., Abrantes, D.P., Brasileiro, P.S., Bahia, R.G., Leal, R.N., Kaufman, L., Kleypas, J.A., Farina, M., Thompson, F.L., 2012. Rhodolith beds are major CaCO3 biofactories in the tropical South West Atlantic. PloS One 7, 0035171.

Amao, A.O., Kaminski, M.A., Setoyama, E., 2016. Diversity of foraminifera in a shallow restricted lagoon in Bahrain. Micropaleontology 62, 197–211.

Bandeira-Pedrosa, M.E., Pereira, S.M.B., Oliveira, E.C., 2004. Taxonomy and distribution of the green algal genus *Halimeda* (Bryopsidales, Chlorophyta) in Brazil. Braz. J. Botany 27, 363–377.

Beavington-Penney, S.J., Racey, A., 2004. Ecology of extant nummulitids and other larger benthic foraminifera: applications in palaeoenvironmental analysis. Earth Sci. Rev. 67, 219–265.

Beavington-Penney, S.J., Wright, V.P., Racey, A., 2005. Sediment production and dispersal on foraminifera-dominated early Tertiary ramps: the Eocene El Garia Formation, Tunisia. Sedimentology 52, 537–569.

Beavington-Penney, S.J., Wright, V.P., Racey, A., 2006. The middle Eocene Seeb Formation of Oman: an investigation of acyclicity, stratigraphic completeness, and accumulation rates in shallow marine carbonate settings. J. Sediment. Res. 76, 1137–1161.

Bieda, F., 1963. Larger foraminifers of the Tatra Eocene. Institut Geologiczny Prace 37, 157–215.

Blendinger, W., Blendinger, E., 1989. Windward-leeward effects on Triassic carbonate bank margin facies of the Dolomites, northern Italy. Sedimentary Geol. 64, 143–166.

BouDagher-Fadel, M.K., Price, G.D., Hu, X., Li, J., 2015. Late Cretaceous to early Paleogene foraminiferal biozones in the Tibetan Himalayas, and a pan-Tethyan foraminiferal correlation scheme. Stratigraphy 12, 67–91.

Brandano, M., Frezza, V., Tomassetti, L., Pedley, M., Matteucci, R., 2009. Facies analysis and palaeoenvironmental interpretation of the late Oligocene Attard Member (lower Coralline Limestone Formation), Malta. Sedimentology 56, 1138–1158.

Brandano, M., Tomassetti, L., Frezza, V., 2015. *Halimeda* dominance in the coastal wedge of Pietra di Finale (Ligurian Alps, Italy): The role of trophic conditions. Sediment. Geol. 320, 30–37.

Brasier, M.D., 1975. The ecology and distribution of recent foraminifera from the reefs and shoals around Barbuda, West Indies. J. Foraminiferal Res. 5, 193–210.

Chablais, J., Onoue, T., Martini, R., 2010. Upper Triassic reef-limestone blocks of southwestern Japan: new data from a Panthalassan seamount. Palaeogeogr. Palaeoclimatol. Palaeoecol. 293, 206–222.

Chan, S.A., Kaminski, M.A., Al-Ramadan, K., Babalola, L.O., 2017. Foraminiferal biofacies and depositional environments of the Burdigalian mixed carbonate and siliciclastic Dam Formation, Al-Lidam area, Eastern Province of Saudi Arabia. Palaeogeogr. Palaeoclimatol. Palaeoecol. 469, 122–137.

Dasgupta, A.B., 1977. Geology of Assam-Arakan region. Quart. J. Geol. Mining Metallurg. Soc. India 49, 1–54.

Drobne, K., Cosovic, V., Moro, A., Buckovic, D., 2011. The role of the Palaeogene Adriatic Carbonate Platform in the spatial distribution of Alveolinids. Turkish J. Earth Sci. 20, 721–751.

Dutta, S.K., Jain, K.P., 1980. Geology and Palynology of the area around Lumshnong, Jaintia Hills, Meghlaya, India. Biol. Mem. 5, 56–81.

Eder, W., Hohenegger, J., Briguglio, A., 2016. Depth-related morphoclines of megalospheric tests of *Heterostegina depressa* D' Orbigny: Biostratigraphic and paleobiological implications. Palaios 32, 110–117.

Eder, W., Hohenegger, J., Briguglio, A., 2018. Test flattening in the larger foraminifer *Heterostegina depressa*: predicting bathymetry from axial sections. Paleobiology 44, 76–88.

Eldrett, J.S., Greenwood, D.R., Harding, I.C., Huber, M., 2009. Increased seasonality through the Eocene to Oligocene transition in northern high latitudes. Nature 459, 969–973.

Geel, T., 2000. Recognition of stratigraphic sequences in carbonate platform and slope deposits: empirical models based on microfacies analysis of Palaeogene deposits in southeastern Spain. Palaeogeogr. Palaeoclimatol. Palaeoecol. 155, 211–238.

Ghose, B.K., 1976. Palaeogene reef rock-complex of Meghalaya and its oil potentialities. Sci. Cult. 42, 248–253.

Goeting, S., Briguglio, A., Eder, W., Hohenegger, J., Roslim, A., Kocsis, L., 2018. Depth distribution of modern larger benthic foraminifera offshore Brunei Darussalam. Micropaleontology 64, 299–316.

Gonera, M., 2012. Palaeoecology of the Middle Miocene foraminifera of the Nowy Sącz Basin (Polish Outer Carpathians). Geol. Quart. 56, 107–116.

Govindan, A., 2003. Tertiary larger foraminifera in Indian basins: A tie up with Standard Planktic Zones and Letter Stages. Gondwana Geol. Mag. Spec. Vol. 6, 45–78.

Greenwood, D.R., Wing, S.L., 1995. Eocene continental climates and latitudinal temperature gradients. Geology 23, 1044–1048.

Hadi, M., Mosaddegh, H., Abbassi, N., 2016. Microfacies and biofabric of nummulite accumulations (Bank) from the Eocene deposits of western Alborz (NW Iran). J. Afr. Earth Sci. 124, 216–233.

Hadi, M., Vahidinia, M., Hrabovsky, J., 2018. Larger foraminiferal biostratigraphy and microfacies analysis from the Ypresian (Ilerdian-Cuisian) limestones in the Sistan Suture Zone (eastern Iran). Turkish J. Earth Sci. 27, http://dx.doi.org/10.3906/yer-1802-10.

Hallock, P., 1985. Why are larger foraminifera large? Paleobiology 11, 195–208.

Hallock, P., Glenn, E.C., 1986. Larger foraminifera: a tool for paleoenvironmental analysis of Cenozoic carbonate depositional facies. Palaios 1, 55–64.

Hallock, P., Schlager, W., 1986. Nutrient excess and the demise of coral reefs and carbonate platforms. Palaios 1, 389–398.

Hohenegger, J., 1994. Distribution of living larger foraminifera NW of Sesoko-Jima, Okinawa, Japan. Mar. Ecol. 15, 291–334.

Hohenegger, J., 2004. Depth coenoclines and environmental considerations of western Pacific larger foraminifera. J. Foraminiferal Res. 34, 9–33.

Hohenegger, J., 2005. Estimation of environmental paleogradient values based on presence/absence data: a case study using benthic foraminifera for paleodepth estimation. Palaeogeogr. Palaeoclimatol. Palaeoecol. 217, 115–130.

Hohenegger, J., 2009. Functional shell geometry of symbiont-bearing benthic foraminifera. J. Coral Reef Stud. 11, 81–89.

Hottinger, L., 1960. Recherches sur les alvéolines du Paléocène et de l'Éocène. Mem. Suisses Paleontol. 75/76, 1–243.

Hottinger, L., 1977. Distribution of larger Peneroplidae, *Borelis* and Nummulitidae in the Gulf of Elat, Red Sea. Utrecht Micropaleontol. Bull. 15, 35–109.

Hottinger, L., 1982. Larger Foraminifera, giant cells with a historical background. Naturwissenschaften 69, 361–371.

Hottinger, L., 1983. Processes determining the distribution of larger foraminifera in space and time. Utrecht Micropaleontol. Bull. 30, 239–253.

Hottinger, L., 1997. Shallow benthic foraminiferal assemblages as signals for depth of their deposition and their limitations. Bull. Soc. geol. France 168, 491–505.

Hottinger, L., Drobne, K., 1988. Tertiary alveolinids: problems linked to the conception of species. Rev. Paleobiol. (Benthos'86) 2, 665–681.

Hottinger, L., Halicz, E., Reiss, Z., 1993. Recent Foraminiferida from the Gulf of Aqaba, Red Sea. Dela SAZU, Ljubljana (33, 179 p.).

Huber, M., Caballero, R., 2011. The early Eocene equable climate problem revisited. Clim. Past 7, 603–633.

Ionesi, L., 1971. Le Flysch paléogène de la vallée de la Moldova. Editura Academiei Republicii Socialiste Romaniâ, Bucharest (250 p.).

Jauhri, A.K., 1994. Carbonate buildup in the Lakadong Formation of the South Shillong Plateau, NE India: A micropaleontological perspective. In: Matteucci, R., et al. (Eds.), Studies on Ecology and Paleoecology of Benthic Communities. Boll. Soc. Paleontol. It. 2, 157–169.

Jauhri, A.K., 1997. Post-Cretaceous record of larger foraminifera from the Shillong Plateau, India: an evidence of environmental recovery during Early Cenozoic. Palaeobotanist 46, 118–126.

Jauhri, A.K., 1998. *Miscellanea* (Foraminiferida) from the South Shillong region, NE India. J. Palaeontol. Soc. India 43, 73–83.

Jauhri, A.K., Agarwal, K.K., 2001. Early Palaeogene in the south Shillong Plateau, NE India: local biostratigraphic signals of global tectonic and oceanic changes. Palaeogeogr. Palaeoclimatol. Palaeoecol. 168, 187–203.

Kalita, K.D., Gogoi, H., 2015. Microfacies types (MFT) and Palaeoenvironment of the Umlatodoh Carbonates in the Shillong Plateau of Meghalaya, NE India. J. Geol. Soc. India 85, 686–696.

Kiessling, W., Flügel, E., Golonka, J., 2003. Patterns of Phanerozoic carbonate platform sedimentation. Lethaia 36, 195–226.

Langer, M.R., Hottinger, L., 2000. Biogeography of selected "larger" foraminifera. Micropaleontology 46, 105–126.

Lees, A., 1975. Possible influence of salinity and temperature on modern shelf carbonate sedimentation. Mar. Geol. 19, 159–198.

Loucks, R.G., Moody, R.T.J., Bellis, J.K., Brown, A.A., 1998. Regional depositional setting and pore network systems of the El Garia Formation (Metlaoui Group, Lower Eocene), offshore Tunisia. In: MacGregor, D.S., Moody, R.T.J., Clark-Lowes, D.D. (Eds.) Petroleum Geology of North Africa. Geol. Soc. Lond., Spec. Publ. 132, 355–374.

Massieux, M., 1973. Micropaléontologie stratigraphique de l'Éocène des Corbières septentrionales (Aude). Centre national de la recherche scientifique, Paris (146 p.).

Matsumaru, K., 1996. Tertiary larger foraminifera (Foraminiferida) from the Ogasawara Islands, Japan. Palaeontol. Soc. Jpn. Spec. Papers 36, 1–239.

Matsumaru, K., Sarma, A., 2010. Larger foraminiferal biostratigraphy of the lower Tertiary of Jaintia Hills, Meghalaya, NE India. Micropaleontology 56, 539–565.

Molina, E., Canudo, J.I., Guernet, C., McDougall, K., Ortiz, N., Pascual, J.O., Pares, J., Samso, J.M., Serra-Kiel, J., Tosquella, J., 1992. The stratotypic Ilerdian revisited: integrated stratigraphy across the Paleocene/Eocene boundary. Rev. Micropaleontol. 35, 143–156.

Murray, J.W., 1991. Ecology and Paleoecology of Benthic Foraminifera. Routledge (341 p.).

Murray, J.W., 2006. Ecology and applications of benthic foraminifera. Cambridge University Press (426 p.).

Murty, K.N., 1983. Geology and hydrocarbon prospects of Assam shelf–recent advances and present status. In: Bhandari, L.L. (Ed.) Petroliferous basins of India. Petroleum Asia J. 6, 1–14.

Nagappa, Y., 1959. Foraminiferal biostratigraphy of Cretaceous-Eocene succession in the India-Pakistan-Burma region. Micropaleontology 5, 141–181.

Özgen-Erdem, N., İnan, N., Akyazı, M., Tunoğlu, C., 2005. Benthonic foraminiferal assemblages and microfacies analysis of Paleocene–Eocene carbonate rocks in the Kastamonu region, Northern Turkey. J. Asian Earth Sci. 25, 403–417.

Özgen-Erdem, N., Akyazı, M., Karabaşoğlu, A., 2007. Biostratigraphic interpretation and systematics of *Alveolina* assemblages from the Ilerdian–Cuisian limestones of Southern Eskişehir, Central Turkey. J. Asian Earth Sci 29, 911–927.

Papazzoni, C.A., Ćosović, V., Briguglio, A., Drobne, K., 2017. Towards a calibrated larger foraminifera biostratigraphic zonation: celebrating 18 years of the application of shallow benthic zones. Palaios 32, 1–5.

Parker, J.H., Gischler, E., 2015. Modern and relict foraminiferal biofacies from a carbonate ramp, offshore Kuwait, Northwest Persian Gulf. Facies 61, 10.

Pedley, M., 1998. A review of sediment distributions and processes in Oligo-Miocene ramps of southern Italy and Malta (Mediterranean divide). In: Wright, V.P., Burchette, T.P. (Eds.) Carbonate Ramps. Geol. Soc. Lond., Spec. Publ. 149, 163–179.

Perrin, C., Bosence, D., Rosen, B., 1995. Quantitative approaches to palaeozonation and palaeobathymetry of corals and coralline algae in Cenozoic reefs. In: Bosence, D.W.J., Allison, P.A. (Eds.) Marine palaeoenvironmental analysis from fossils. Geol. Soc. Lond., Spec. Publ. 83, 181–229.

Pomar, L., Baceta, J.I., Hallock, P., Mateu-Vicens, G., Basso, D., 2017. Reef building and carbonate production modes in the west-central Tethys during the Cenozoic. Mar. Petrol. Geol. 83, 261–304.

Pujalte, V., Caballero, J.I.B., Schmitz, B., Orue-Etxebarria, X., Agirre, A.P., Bilbao, G.B., Ingunza, E.A., Santamaria, F.C., Moreno, A.R., Serra-Kiel,

J., Angrill, J.T., 2009. Redefinition of the Ilerdian stage (early Eocene). Geol. Acta 7, 177–194.

Quaranta, F., Tomassetti, L., Vannucci, G., Brandano, M., 2012. Coralline algae as environmental indicators: a case study from the Attard member (Chattian, Malta). Geodiversitas 34, 151–166.

Racey, A., 1995. Lithostratigraphy and larger foraminiferal (nummulitid) biostratigraphy of the Tertiary of northern Oman. Micropaleontology 41, 1–123.

Racey, A., 2001. A review of Eocene nummulite accumulations: structure, formation and reservoir potential. J. Pet. Geol. 24, 79–100.

Rasser, M.W., Scheibner, C., Mutti, M., 2005. A paleoenvironmental standard section for Early Ilerdian tropical carbonate factories (Corbières, France; Pyrenees, Spain). Facies 51, 218–232.

Renema, W., 2008. Habitat selective factors influencing the distribution of larger benthic foraminiferal assemblages over the Kepulauan Seribu. Mar. Micropaleontol. 68, 286–298.

Reolid, M., Nikitenko, B.L., Glinskikh, L., 2014. *Trochammina* as opportunist foraminifera in the Lower Jurassic from north Siberia. Polar Res. 33, 21653.

Sarkar, S., 2015. Thanetian-Ilerdian coralline algae and benthic foraminifera from northeast India: microfacies analysis and new insights into the Tethyan perspective. Lethaia 48, 13–28.

Sarkar, S., 2016. Early Eocene calcareous algae and benthic foraminifera from Meghalaya, NE India: A new record of microfacies and palaeoenvironment. J. Geol. Soc. India 88, 281–294.

Sarkar, S., 2017a. Microfacies analysis of larger benthic foraminifera-dominated Middle Eocene carbonates: a palaeoenvironmental case study from Meghalaya, N-E India (Eastern Tethys). Arab. J. Geosci. 10, 21.

Sarkar, S., 2019. Does specialization imply rare fossil records of some benthic foraminifera: Late Palaeocene examples from the eastern Neo-Tethys (Meghalaya, NE India). Palaeogeogr. Palaeoclimatol. Palaeoecol. 514, 124–134.

Sarma, A., Ghosh, A.K., Sarkar, S., 2014. First record of coralline red algae from the Kopili Formation (late Eocene) of Meghalaya, NE India. Natl Acad. Sci. Lett. 37, 503–507.

Schaub, H., 1981. Nummulites et Assilines de la Téthys paléogène. Taxonomie, Phylogenèse et biostratigraphie. Mem. Soc. Paleontol. Suisse (104/105/106, 236 p.).

Scheibner, C., Speijer, R.P., 2009. Recalibration of the Tethyan shallow-benthic zonation across the Paleocene–Eocene boundary: the Egyptian record. Geol. Acta 7, 195–214.

Scheibner, C., Speijer, R.P., Marzouk, A., 2005. Larger foraminiferal turnover during the Paleocene/Eocene Thermal Maximum and paleoclimatic control on the evolution of platform ecosystems. Geology 33, 493–496.

Scheibner, C., Rasser, M.W., Mutti, M., 2007. The Campo section (Pyrenees, Spain) revisited: Implications for changing benthic carbonate assemblages across the Paleocene–Eocene boundary. Palaeogeogr. Palaeoclimatol. Palaeoecol. 248, 145–168.

Serra-Kiel, J., Hottinger, L., Caus, E., Drobne, K., Ferrandez, C., Jauhri, A.K., Less, G., Pavlovec, R., Pignatti, J., Samso, J.M., Schaub, H., 1998. Larger foraminiferal biostratigraphy of the Tethyan Paleocene and Eocene. Bull. Soc. geol. France 169, 281–299.

Severin, K.P., Lipps, J.H., 1989. The weight-volume relationship of the test of *Alveolinella quoyi*: Implications for the taphonomy of large fusiform foraminifera. Lethaia 22, 1–12.

Španiček, J., Ćosović, V., Mrinjek, E., Vlahović, I., 2017. Early Eocene evolution of carbonate depositional environments recorded in the Čikola Canyon (North Dalmatian Foreland Basin, Croatia). Geol. Croat. 70, 11–25.

Tomassetti, L., Benedetti, A., Brandano, M., 2016. Middle Eocene seagrass facies from Apennine carbonate platforms (Italy). Sediment. Geol. 335, 136–149.

Torres-Silva, A.I., Eder, W., Hohenegger, J., Briguglio, A., 2019. Morphometric analysis of Eocene nummulitids in western and central Cuba: taxonomy, biostratigraphy and evolutionary trends. J. Syst. Palaeontol. 17, 557–595.

Webster, J.M., Clague, D.A., Braga, J.C., Spalding, H., Renema, W., Kelley, C., Applegate, B., Smith, J.R., Paull, C.K., Moore, J.G., Potts, D., 2006. Drowned coralline algal dominated deposits off Lanai, Hawaii: carbonate accretion and vertical tectonics over the last 30 ka. Mar. Geol. 225, 223–246.

Wilson, M.E.J., Vecsei, A., 2005. The apparent paradox of abundant foramol facies in low latitudes: their environmental significance and effect on platform development. Earth Sci. Rev. 69, 133–168.

Wing, S.L., Alroy, J., Hickey, L.J., 1995. Plant and mammal diversity in the Paleocene to early Eocene of the Bighorn Basin. Palaeogeogr. Palaeoclimatol. Palaeoecol. 115, 117–155.

Wray, J.L., 1977. Calcareous Algae. Elsevier Publishers, Amsterdam (190 p.).

Yordanova, E.K., Hohenegger, J., 2002. Taphonomy of larger foraminifera: Relationships between living individuals and empty tests on flat reef slopes (Sesoko Island, Japan). Facies 46, 169.

Zachos, J.C., Dickens, G.R., Zeebe, R.E., 2008. An early Cenozoic perspective on greenhouse warming and carbon-cycle dynamics. Nature 451, 279–283.

Zamagni, J., Mutti, M., Košir, A., 2008. Evolution of shallow benthic communities during the Late Paleocene–earliest Eocene transition in the northern Tethys (SW Slovenia). Facies 54, 25.

Zhang, Q., Willems, H., Ding, L., 2013. Evolution of the Paleocene-Early Eocene larger benthic foraminifera in the Tethyan Himalaya of Tibet, China. Int. J. Earth Sci. 102, 1427–1445.

Zhang, Q., Willems, H., Ding, L., Xu, X., 2018. Response of larger benthic foraminifera to the Paleocene–Eocene thermal maximum and the position of the Paleocene/Eocene boundary in the Tethyan shallow benthic zones: Evidence from South Tibet. GSA Bull. 131, 84–98.